Fabrication of homogenous pellets by freeze granulation of optimized TiO_2-Y_2O_3 suspensions

F. La Lumia, L. Ramond, C. Pagnoux, G. Bernard-Granger

Fabrication of homogenous pellets by freeze granulation of optimized TiO_2-Y_2O_3 suspensions

F. La Lumia [a], L. Ramond [a], C. Pagnoux [b], G. Bernard-Granger [a]*

[a] CEA, Nuclear Energy Division, Research Department on Mining and Fuel Recycling Processes, SFMA, BP 17171, F-30207 Bagnols sur Cèze, France

[b] Institute of Research for Ceramics (IRCER), 12 rue Atlantis, F-87068 Limoges, France

* Corresponding author. Phone: +33 466797466 Email: guillaume.bernard-granger@cea.fr Address: Bât. 397 SFMA/DIR, BP 17171, F-30207 Bagnols sur Cèze, France

Keywords: Suspension, granulation, freeze drying

Abstract

The development of Generation IV sodium-cooled fast reactors (SFR) is currently studied by several countries, France in particular. To manufacture the MOX fuels for these new types of reactors, innovative wet colloidal processes are investigated. Among these processes, freeze granulation of water-based powder suspension seems a promising way to yield homogenous and easy-to-press mixed UO_2-PuO_2 granules. These granulated powders are expected to form dense, homogenous and flaw-free pellets by uniaxial pressing. Properties of the granulated powder and subsequent pellet are heavily affected by the suspension formulation and atomization conditions. Therefore, these conditions must be studied and optimized to ensure the production of granules with good processability and thus compliant final MOX fuel pellets with the required density, homogeneity, mechanical strength and absence of defects. In this scope, the freeze granulation process was investigated by the use of UO_2 and PuO_2 surrogating (i.e. mimicking) powders, TiO_2 and Y_2O_3 respectively.

1. Introduction / Objectives

The current manufacturing of UO_2-PuO_2 MOX fuel pellets is carried out by a dry route process [1], through steps involving fine powders (grinding, mixing and pressing). In order to limit powder dissemination and to improve the processability (flowability and pressability) of the UO_2-PuO_2 powder mix, new wet colloidal routes are investigated. One of those is the freeze granulation process (Fig. 1). This process [2,3,4] implies to prepare a concentrated, water-based powder suspension which is then atomized into small droplets through a spraying nozzle. Suspension droplets are sprayed into liquid nitrogen under stirring and are instantly frozen. The resulting frozen granules are recovered and subsequently freeze-dried under vacuum to sublimate the ice they contain and yield a dry granulated powder.

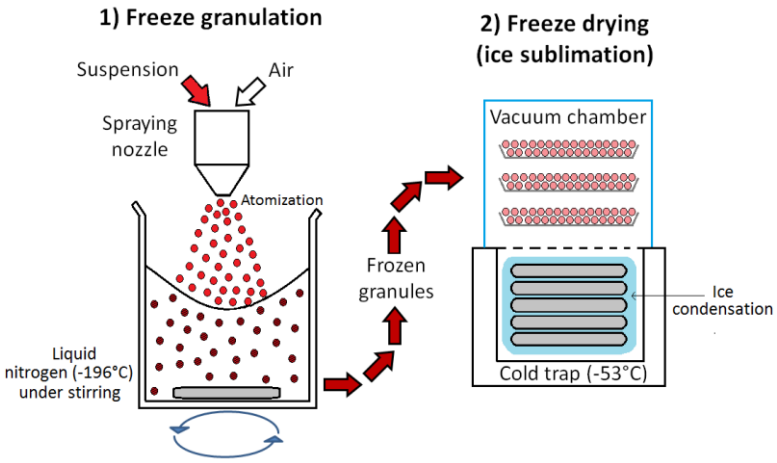

Fig. 1: Principle of the freeze granulation process.

This process has several advantages compared to the more classical spray-drying process [5]. These advantages include good control of granule density, the absence of cavities in the granules, as well as a high degree of granule homogeneity. Indeed, droplet freezing is a fast process, unlike the water evaporation step of the spray-drying process. Thus, there is not any migration (by capillary action) of small particles or binder taking place in the droplet. Consequently, the homogeneity is retained in the final freeze-dried granules [3,4,6]. Additionally, the spray-drying process implies granule shrinkage and even sometimes deformation during the water removal step. It is not the case during the freeze granulation process, due to the rapidity of the freezing. Thus, during freeze granulation, the granules maintain their spherical shape and homogeneity. This grants respectively higher granule flowability and deformability compared to spray drying, with whom inflation defects persist as large voids in the interior of the granule [7]. Those imperfections may resist compaction and also be present in the compacted specimens. Finally, compared to spray-drying, freeze granulation is able to yield granules with better sphericity and more homogenously distributed intra-granular porosity and additives. This respectively ensures a better flowability and crushability of the granules, granting the freeze granulated powder a better pressability (i. e. shaping by pressing).

Taking into account all the above-mentioned characteristics of the freeze granulation process, the present study focuses on the application of this process to the formation of nuclear MOX fuel pellets, from the raw powders to the final dense pellets. For easier handling and processing during the investigation, experiments were made at first with surrogate powders, i.e. non-radioactive powders which have some physicochemical properties similar to those of the radioactive powders UO_2 and PuO_2. To select each surrogating powder, properties considered are the ones which are relevant of the freeze granulation process. This process implies powders suspended in aqueous media at high concentrations. Thus, the UO_2 and PuO_2 powders properties to mimic are the following:

- the size and morphology of the powder particles, which are related to the suspension rheology,
- the isoelectric point (PIE) of the materials, which are related to the electrokinetic properties of the particles in suspension (i. e. particle surface charge).

Thus, according to these criteria, the surrogate powders chosen for this study were TiO_2 and Y_2O_3, selected for their suspension properties (isoelectric point and particle morphology) to surrogate UO_2 and PuO_2, respectively.

The aim of the research reported in this paper was to determine how to prepare, from the raw TiO_2 and Y_2O_3 powders, dense, flaw-free, homogenous and resistant TiO_2-Y_2O_3 pellets by the freeze granulation process. The preparation and dispersion of concentrated, water-based TiO_2-Y_2O_3 suspensions have already been investigated and optimized in a previous paper by the same authors.

The aims were to ensure a high solid loading and stability (settling resistance) of the suspension, as well as a viscosity low enough to allow the suspension to be sprayed into droplets.
The surrogate powders TiO_2 and Y_2O_3 were studied mixed together in proportions of 15 at% Y (Y/(Y+Ti) = 0.15). Such proportions were chosen to represent a trade-off between the atomic percent of Pu in the light water reactor MOX fuels (3-10 at% Pu) and in the fuels envisaged for Generation IV fast neutron reactors (20-30 at% Pu).

2. Experimental section

2.1 Analytical devices and techniques

2.1.1 Raw powders characterization devices

Specific surface areas were assessed with BET (Bruauer, Emett, Teller) N_2 sorption method with a Micromeritics ASAP 2020 surface area analyzer. Densities were measured with a Micromeritics AccuPyc 1340 helium pycnometer. Particle morphologies were determined using a Cambridge Instruments Stereoscan S 260 Scanning Electron Microscope (SEM). Particle size distributions of raw powders were measured with a Horiba LA-950 liquid granulometer and calculated using the Mie diffraction theory. In order to prevent particle agglomeration during measurements, 0.5 wt% of Darvan CN dispersant was added to the powder suspensions 15 min before measurements. Moreover, suspensions were ultrasonicated for 30 s prior to the measurements.

2.1.2 Granules and pellets characterization devices

Granules size distributions were assessed with a Malvern MasterSizer 2000 dry-route granulometer and calculated using the Mie diffraction theory. Granules internal porosity was measured with a mercury intrusion porosimeter (MIP). Pore size distributions were computed to account only for the intragranular porosity, disregarding the intergranular porosity (cut-off at sizes above 5 µm). Granules flowability was assessed by the measurement of their bulk (tapped and untapped) density, using a vibrating table (tap densitometer). Granules and pellets micrographs and chemical cartographies were obtained with a JEOL IT300 SEM equipped with an Oxford Instruments EDS (Electron Diffraction Spectroscopy) analysis module.

2.1.3 Suspensions preparation

TiO_2-Y_2O_3 suspensions for rheology and freeze granulation experiments were prepared with various solid contents in the range 25 - 40 %v by mixing water with dispersant in a flask and then raw powders were added under mechanical stirring. Eventually, enough yttria-stabilized zirconia grinding balls (diameters 3/10/15 mm in volume proportions of 70/10/20) were added to outcrop at the suspension surface. Then, the suspension was let to roll for 20 hrs on a roller mixer (RM-5, CAT) at 15 rpm. This process is known in literature to yield low viscosity suspensions [8,9]. Hereafter, binder(s) were added and the suspension was let to roll for 2 more hours. Finally, the suspension was degassed with a Thinky ARE-250 (Intertronics) planetary mixing and degassing machine for 3 min at 1100 rpm to remove the eventual air bubbles entrapped in the suspension. All the TiO_2-Y_2O_3 suspensions referred to in this paper contain 15 at% Y, where this percentage is expressed in terms of Y atoms among Ti and Y atoms, i. e. Y/(Y+Ti) = 0.15.

2.1.3 Acoustophorometer

Zeta potential measurements were conducted as a function of the pH on the raw materials dispersed at 1.25 %v. in deionized water with an ESA analyser (AcoustoSizer II S flow through system, Colloidal Dynamics). Zeta potential measurements at different pH were made with the automated AcoustoSizer II pH titration system using 1.0 mol/L sodium hydroxide or 1.0 mol/L hydrochloric acid solutions. The starting pH was the natural pH of the suspension (represented by hollow dots on titration curves) before any acid or base addition. pH titrations were made starting from the suspension natural pH to acid or basic pH by adding either hydrochloric acid or sodium hydroxide, respectively. All zeta potential measurements were performed with 10^{-2} mol/L sodium chloride as background electrolyte to keep the ionic strength constant through the whole investigated pH range (7-12). All suspensions for acoustophorometric measurements were prepared with 1.25 %v solid content. First, distilled water and dispersant were mixed under magnetic stirring for 60 s, then oxide powders were added while stirring for further 5 min. Hereafter the suspension was ultrasonicated with an ultrasonic probe (Vibra-cell 75041, BioBlock Scientific) for 2 min to break particle agglomerates. Finally, the suspension was let for 15 min on a roller mixer (CAT, RM-5, Germany) operating at 15 rpm.

2.1.4 Rheometer

A Rheolab QC rheometer (Anton Paar) equipped with a CC27 cylindrical geometry and thermostated at 20°C, was used to assess suspension viscosity. Prior to the measurements, a constant shear rate of 1500 s^{-1} was applied for 120 s to bring each sample to the same rheological past and thus grant measurement reproducibility [10,11]. Rheology measurements were conducted with a ramp of shear rate from 1 to 1500 s^{-1} imposed to the sample, with 30 s delay between each point to let time for steady state to establish. Each experiment of shear rate ramp lasted 10 min, for a total of 20 points acquired per experiment.

2.1.5 Freeze granulation and freeze-drying (lyophilization)

The freeze granulator used for the experiments was a PowderPro LS-2 (PowderPro AB, Sweden). This apparatus was used as received, equipped with the suspension flow regulating device provided with the apparatus. The atomization gas used was air. The suspension and air flow rates injected in the spraying nozzle can be adjusted at the desired values. Unless otherwise stated, the atomization conditions performed were: air pressure of 0.2 bar and suspension flow rate of 33 mL/min (suspension pumped through a peristaltic pump). The rotation speed of the magnetic stirrer in the liquid nitrogen was set at 350 rpm. Immediately after formation, frozen granules were freeze-dried in a Christ Alpha 2-4 LD Plus freeze-drier during 20 hrs under a final vacuum of 10^{-3} mbar.

2.1.6 Pressing and sintering

Granulated powders were shaped into pellets by uniaxial pressing using a custom-made electromechanical press (Champalle, France) with floating die. Applied pressure was set at 190 MPa, the compression speed was set at 10 mm/s and the holding time at 3.0 s. The external parts of the die were lubricated with a stearic acid solution.
Raw pellets were sintered using a Nabertherm LH 04-17 furnace. The pellets were sintered under air at 1500°C during 1.5 hrs, after a heating rate of 30°C/min, without debinding step.

2.2 Raw chemicals

Darvan CN (Vanderbilt Minerals LLC) was used as a dispersant, in the form of a ready-to-use 25 wt% aqueous solution. This polymer is an ammonium polymethyl methacrylate with an average molar weight of 15,000 g/mol.

Polyethylene glycols (PEGs) of several molecular weights (300, 3400 and 6000 g/mol) were used as binders (Sigma-Aldrich, Inc) directly in their pure forms (liquid state for PEG 300 and pulverulent solid state for all other PEGs).
Polyvinyl alcohols (PVA) of several molecular weights and hydrolysis rates (22,000 g/mol, 99 % hydrolyzed and 31,000 g/mol, 88 % hydrolyzed) were used as binders (Sigma-Aldrich, Inc.). Both were used in the form of a 10 wt% aqueous solution, prepared freshly before use by dissolution of the proper amount of PVA powder into distilled water under magnetic stirring and gentle heating until complete dissolution.
Dispersant and binder concentrations will be expressed in wt% of the dry powder present in the considered suspension.

3 Results and discussion

3.1 Raw powders characteristics

The main features of the surrogate and active powders are compared and summarized in Table 1. The TiO_2 and Y_2O_3 surrogate powders have most of their suspension-relevant characteristics (i. e. IEP, particle morphology and size distribution) close to the radioactive powders UO_2 and PuO_2, respectively. However, the surrogate powders densities are 2 to 3 times lower than the active powders densities. The powder density obviously plays an important role in particle settling rate (and thus suspension stability) when suspended in liquid media. Indeed, UO_2 and PuO_2 powders are very dense and it was practically impossible to find commercial surrogate powders with such high densities, while having their other main suspension-relevant properties (i. e. IEP, particle morphology and size distribution) close to the ones of the radioactive powders. Thus, TiO_2 and Y_2O_3 powders appeared to be the best trade-off between all the suspension-relevant characteristics of the radioactive powders to surrogate.

Powder formula	Supplier, reference	Purity (%)	Particle size (µm)	Particle morphology	Density ($g.cm^{-3}$)	Specific surface area ($m^2.g^{-1}$)	Expected isoelectric point (from literature)	SEM micrography
UO_2 (dry route process)	N/A	N/A	0.1 + 0.8	Nanosphere aggregates	10.97	2	5.5 [12,13]	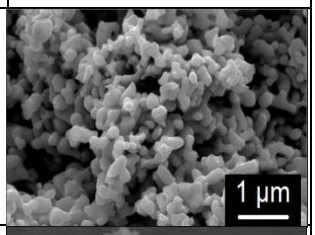
TiO_2	Marion Technologie	99.9	0.07 + 0.8		3.78	12	5.5 [13,14]	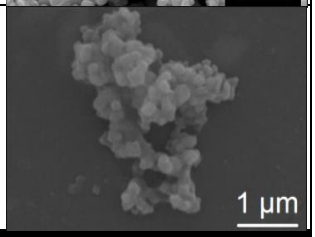
PuO_2	N/A	N/A	1 to 10	Platelets	11.5	6	9 [13]	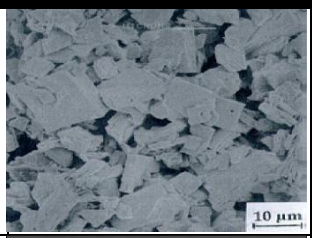
Y_2O_3	HC.Starck grade C	99.95	0.25 + 1 to 7		5.01	14	9 [13,15]	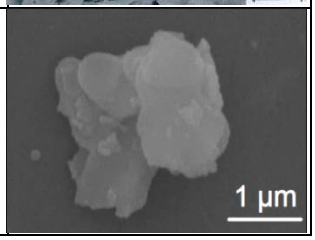

Table 1: Main characteristics of the active powders UO_2, PuO_2 and their respective surrogating powders TiO_2 and Y_2O_3.

3.2 Suspension formulation and rheology

The preparation process and co-dispersion (using Darvan CN polymethacrylate dispersant) of the TiO_2 - Y_2O_3 suspensions were studied in detail in a previous paper by the same authors [16]. It was highlighted that in order to have concentrated, yet low viscous TiO_2 - Y_2O_3 suspension, the optimal amount of Darvan CN to use is about 0.5 wt% of the total solid content of the suspension.
However, the impact of binders on the TiO_2 - Y_2O_3 suspension viscosity must also be investigated to ensure that the suspension viscosity remains low enough to allow spraying, even in the presence of binder in the suspension formulation. The usual upper viscosity limit for sprayability is about 250-300 mPa.s [17,18]. In this scope, viscosity of concentrated TiO_2 - Y_2O_3 suspensions have been assessed in the presence of several polymer organic binders, as shown in Fig. 2. All assessed binders induce an increase of suspension viscosity, especially at low shear rates. This phenomenon can be explained by four factors:

- The adsorption competition between the dispersant and the binder macromolecules: the adsorption of a fraction of the binder macromolecules at the surface of the particle leaves fewer adsorption sites available for the adsorption of the dispersant macromolecules. In other words, the presence of a second adsorbable specie (the binder) displaces the adsorption equilibrium of the dispersant towards the unadsorbed (free) state. As a consequence, the particle surface charge is lower and the ionic strength is higher. Thus, electrostatic repulsion forces are lower and agglomeration is more likely to happen, inducing a viscosity increase at low shear rate. This phenomenon occurs only with binders that are effectively able to adsorb quantitatively onto ceramic particles like PEG [19], but much less with PVA because of its limited ability to adsorb on ceramic particles [10,20,21].

- The depletion flocculation mechanism: Addition of binder macromolecules which do not quantitatively adsorb on ceramic particles (like in the case of PVA macromolecules) increases the concentration of unadsorbed (free) polymer chains in the suspension. These free chains act as a flocculent agent through a depletion flocculation mechanism [22]. In this mechanism, when two particles come close to each other, the free polymer chains remain out of the narrow space between the two particles, inducing a solute concentration gradient and thus an osmotic pressure that drains the solvent out of the space between the particles, making them agglomerate together. It brings the suspension into a flocculated state and thus the low shear viscosity increases. This phenomenon was observed by Khan *et al* for Darvan CN and PVA used in alumina suspensions [10].

- The disruption of the shear plane induced by the adsorbed binder chains: the presence of dispersant macromolecules on the particle surface induces a particular conformation of the adsorbed binder, with a large fraction of absorbed binder chains protruding into the shear-plane layer and away from the particle surface. This disrupts the particle shear plane and thus induces a decrease in electrophoretic mobility. As a result, particles can flocculate easier and low-shear viscosity increases. This phenomenon has been observed and explained in detail for PMMA and PVA (respectively as dispersant and binder) by Paik *et al* [20].

- The presence of free solvated polymer: Addition of binder macromolecules which do not quantitatively adsorb on ceramic particles (like in the case of PVA macromolecules) increases the concentration of unadsorbed (free) polymer chains in the suspension solvent. The presence of these free solvated polymer chains induces an increase of the solvent viscosity, especially for high MW polymer chains like it is the case for PVA 22M in the present work.

Moreover, it appears on Fig. 2 that the higher the PEG MW (molecular weight), the higher the viscosity increases. For PEG binder and zinc oxide particles, Liufu *et al* [19] observed that the total amount of adsorbed PEG increases with molecular weight. This tendency is attributed to the greater participation of loop and tail segments to chain adsorption at the particle-polymer interface. Thus, the amount of dispersant decreases, turning the suspension into a more flocculated state as mentioned above in the first point.

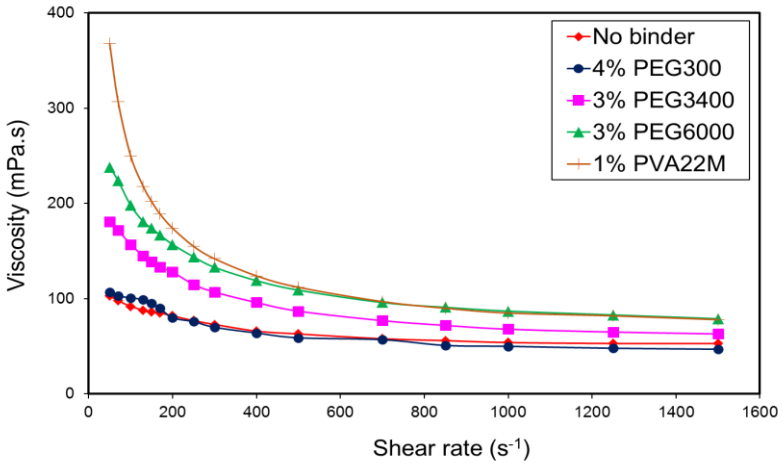

Fig 2: Viscosity of TiO_2-Y_2O_3 suspensions (35 %v total solid loading) containing 0.5 wt% Darvan CN and various binders vs. shear rate.

The observations made from Fig. 2 were confirmed with measurements of the zeta potentials of suspensions containing the same amounts of dispersant (0.5 wt% Darvan CN) and 1 wt% of the aforementioned binders, presented in Fig. 3. It is noticeable that the zeta potentials of suspensions containing PVA 22M or PEG (especially PEG 6000) are less negative than the one without binder. However, that effect is less pronounced for PVA compared to PEG. It was the opposite observation in the case of rheology measurements of Fig. 2. This might indicate that in concentrated suspensions, electrostatic repulsion is not the only particle-particle interaction mechanism affected by the presence of binders. These results also suggest that other mechanisms than the sole adsorption competition between the dispersant and the binder might be at work, like the three others mechanisms listed above.

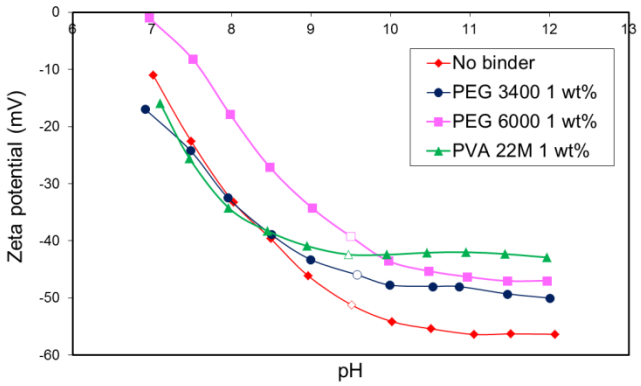

Fig 3: Zeta potentials of TiO_2-Y_2O_3 suspensions (1.25 %v total solid loading) containing 0.5 wt% Darvan CN and various binders vs. pH.

Based on these results, the amount of Darvan CN dispersant used in the suspensions containing PVA binder (both 22M and 31M) was raised in an attempt to counteract the increase of viscosity induced by the presence of the binder. Fig. 3 clearly shows that an amount of 0.75 wt% of Darvan CN dispersant is optimal for suspensions containing 1 wt% PVA 22M binder.

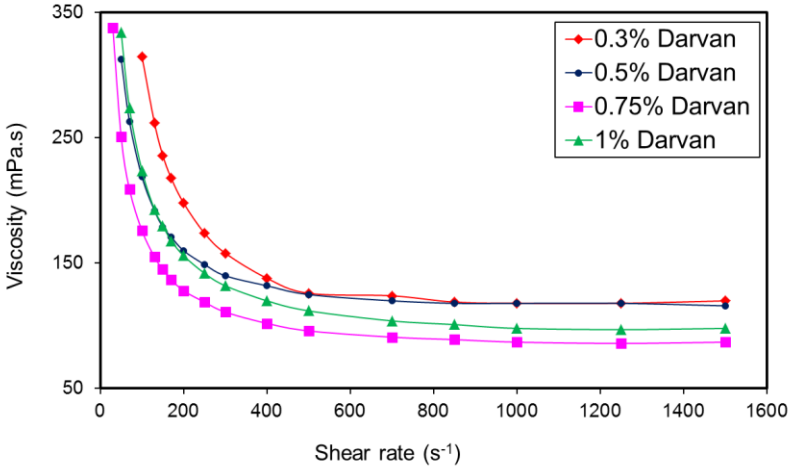

Fig 3: Viscosity of TiO_2-Y_2O_3 suspensions (35 %v total solid loading) containing 1 wt% PVA 22M and various amounts of Darvan CN dispersant vs. shear rate.

3.3 Study of the freeze granulation step

3.3.1 Effects of atomization conditions on granules size distribution and morphology

The effects of suspension viscosity and atomization conditions were assessed on the size distribution and morphology of granules obtained by freeze granulation. Suspensions of different solid loadings and viscosities were freeze-granulated using various atomization conditions. It is clearly visible on Fig. 4 that monomodal size distributions are obtained, regardless of the experimental conditions applied. Fig. 4 also highlights two facts:

- the granule size increases with an increase in suspension flow rate. This effect could by explained considering a defined volume of suspension. The higher its speed of passage in the nozzle, the less it will be dispersed by atomization, which will produce droplets (and thus granules) of higher diameter.
- the granule size decreases with an increase in gas pressure. This could be attributed to transmission of greater energy to the liquid stream passing through the nozzle on increase in gas pressure, which is effective in atomizing the liquid into finer droplets.

Those two effects were already observed in the literature [23,24,25,26]. These results enlighten the fact that acting on the gas and suspension flow rates during suspension atomization is a useful way to tune the granule size.

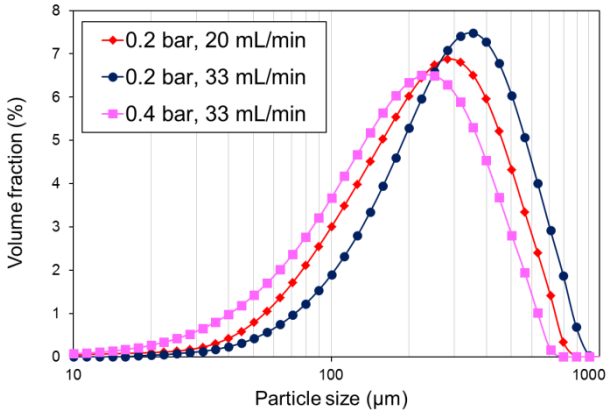

Fig 4: Size distributions of TiO_2-Y_2O_3 granules, obtained from the freeze granulation of suspensions containing 35 %v solid loading, 0.75 wt% Darvan CN, 0.5 wt% PEG3400 and 0.5 wt% PVA 22M.

Suspension viscosity and solid loading also have an influence on granule size, as shown in Fig. 5 and 6 respectively. These figures respectively prove that the granules size increases both with an increase of the suspension solid loading and/or with an increase of the suspension viscosity. As the solid content of suspension increases, the corresponding viscosity of suspension also increases. This explains why the granule size increases with the suspension solid loading. Those facts have already been noticed in the literature by several authors [24,27]. It is intuitive that smaller number of droplets would form by disintegration of a suspension with higher viscosity, as higher amount of resistance will be exerted by such suspension to air in comparison to that of less viscous suspension under given atomization conditions.

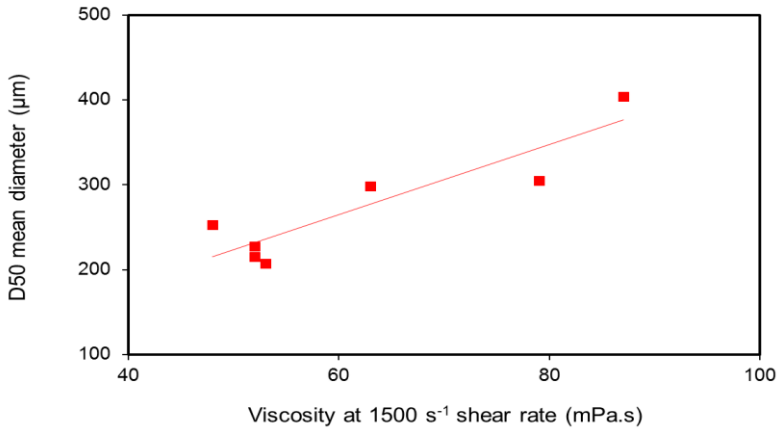

Fig. 5: D50 mean diameter of TiO_2-Y_2O_3 granules (obtained from freeze granulation of suspensions containing 35 %v solid loading, 0.5 wt% Darvan CN and various amounts of binders) as a function of suspension viscosity at 1500 s^{-1} shear rate.

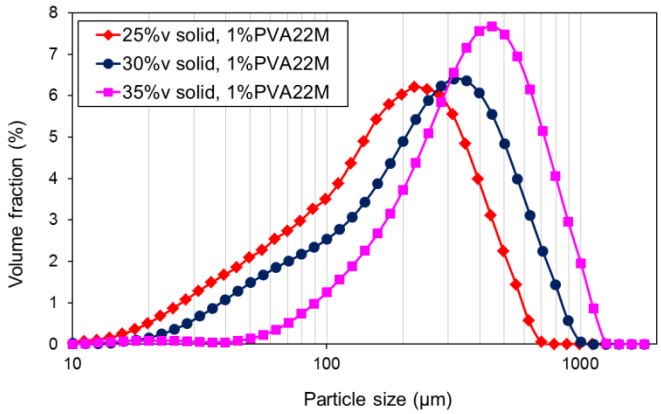

Fig. 6: Size distribution of TiO_2-Y_2O_3 granules, obtained from freeze granulation of suspensions containing 0.75 wt% Darvan CN, 1 wt% PVA 22M and various solid contents.

Moreover, from the freeze granulation experiments performed for the present work, it was also noticed that some experimental conditions during freeze granulation can lead to the formation of misshapen granules. Such granules were obtained when the suspension was too viscous and/or when the air-to-liquid flow rates ratio was too low or too high. These misshapen granules were of two types:

- rod-shaped granules when the suspension viscosity is too high (see Fig. 7 b),
- large granules amalgams/clusters when the flow rates ratio is disproportionate (see Fig. 7 a).

Outside of these conditions, the obtained granules exhibit a spherical shape (see Fig. 7 c and d). The formation of misshapen granules may be explained by two distincts ways.
Formation of rod-like granules depends on the solid concentration and dispersion state of the suspension. If the suspension is too concentrated in solids or not dispersed enough, particle flocs or agglomerates may form respectively due to reduced interparticle distances or insufficient interparticle repulsion forces in the suspension. The atomization of the suspension then occurs not only in the form of droplets but also in the form of needles, arising from atomization of the flocs and can be assimilated to extrusion. Long granules are then obtained, in sticks or needles, as illustrated in Fig. 7 b. Those kind of misshapen granules were also obtained by Barik *et al* [24] because of too high suspension solid content.
Formation of large amalgams of fused granules, as shown in Fig. 7 a, is caused by droplet coalescence, occurring immediately after atomization. This droplet coalescence is due to a too high concentration of droplets in the spray cone and is determined by two factors:

- the suspension and gas flow rates: if the suspension and gas flow rates are both too high, the spray cone will be too concentrated in suspension droplets, increasing their likelihood of going into contact during their flight and resulting in the formation of cluster granules.

- the nozzle design: the spray cone solid angle depends on the nozzle design itself. If this cone solid angle is too low, the concentration of suspension droplets in it will be too high, thus favoring droplet coalescence and hence formation of droplet clusters.

Moreover, the coalescence phenomenon is also influenced by suspension surface tension (which depends itself on the additives present in the suspension). Once again, those kind of misshapen granule clusters were also obtained in previous researches [24,28].

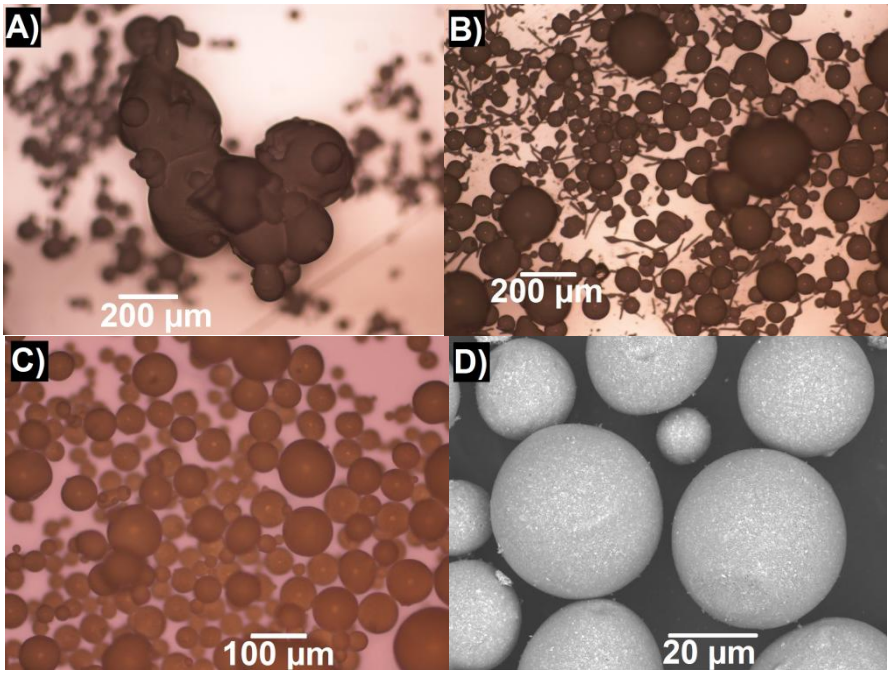

Fig. 7: Examples of TiO_2-Y_2O_3 granules (optical microscope) obtained by freeze granulation under various atomization conditions and suspension viscosities. A: Granule amalgams, B: Rod-shaped granules (among spherical granules), C: Spherical granules, D: Spherical granules (SEM micrograph).

3.3.2 Granules porosity, surface aspect and flowability

Freeze granulation experiments were performed under different conditions to assess the effects of the suspension formulation (solid loading, type and concentration of binders) on several characteristics of the granules: surface aspect, morphology, porosity, chemical homogeneity and flowability.

As previously mentioned, PEG and PVA binders of several MW were used in the formulation of the suspensions intended for freeze granulation. The effects of these binders on the freeze-dried granules were subsequently assessed. It appears that binders with medium of high MW (PEG 3400 and PVA 22M) grant to the granules a smoother surface aspect (Fig. 8) and a narrower size distribution by suppressing (on the size distribution curve) the small secondary bump corresponding to fine granules (Fig. 9). More precisely, PEG 3400 give smooth granules at proportion of 1 to 3 wt% and PVA 22M at proportion around 0.5 wt%, all other conditions remaining unchanged. The presence of such binders in the granules is believed to smoothes the granule surface, probably by sticking the solid elementary particles stronger and closer to each other. This prevents the creation of fines by surface grinding or tearing when granules come into contact [24,29].

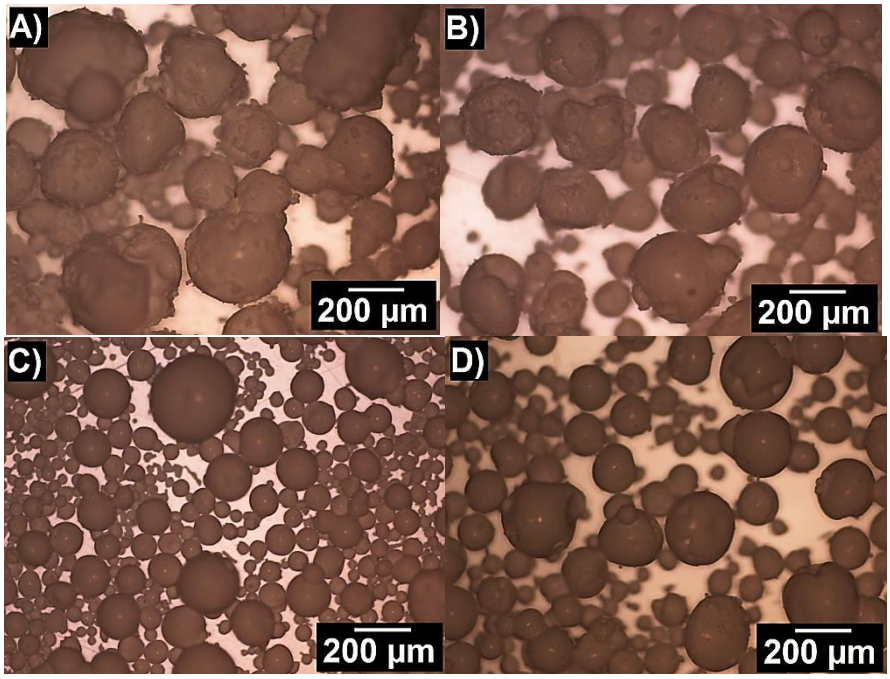

Fig. 8: Optical microscope pictures of TiO_2-Y_2O_3 granules obtained by freeze granulation of suspensions containing 35 %v solid loading, 0.5 wt% Darvan CN and various binders. A: 3 wt% PEG 300, B: 1 wt% PEG 3400, C: 3 wt% PEG 3400, D: 0.5 wt% PVA 22M.

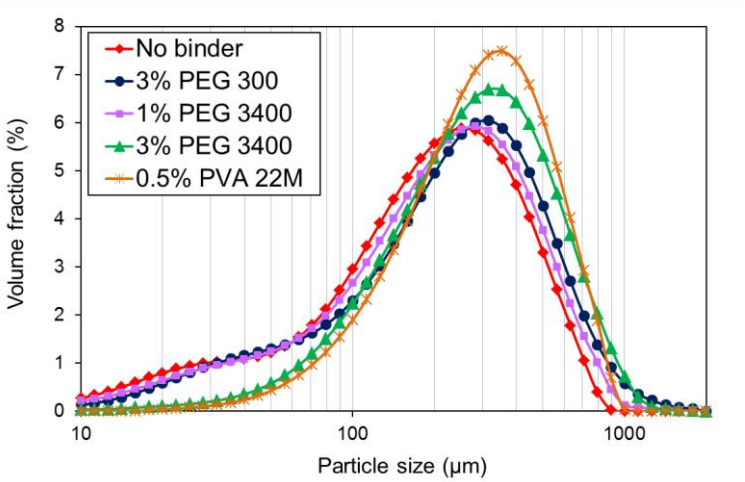

Fig. 9: Size distribution of TiO_2-Y_2O_3 granules, obtained from freeze granulation of suspensions containing 35 %v solid loading, 0.5 wt% Darvan CN and various binders.

Additionally, cross-sectional view SEM micrographics (Fig. 10) of the granules revealed that all granules obtained by freeze granulation have a solid internal structure (no hollow granules). Moreover, granule porosity is heavily influenced by the suspension solid loading. As the suspension solid loading increases, the granule internal total porosity and mean pore size decrease, as shown on Fig. 10 and 11. Those two observations could be explained by the fact that the more concentrated the suspension, the smaller the distance between solid particles and the smaller the ice crystals formed when the suspension droplet goes into liquid nitrogen. Thus, the distance between the powder particles in the frozen granule will be shorter. During ice removal by sublimation, there is no movement/migration of particles taking place [3,4,6]. Thus, the interparticle distance in the freeze-dried granules will also be shorter and so the granule internal porosity will be smaller and its surface will be smoother. This phenomenon has been observed by several authors for the freeze granulation process [17,24,30,31]. Fig. 11 also shows that the pore size (measured by MIP) is centered on 100-200 nm. This value is close to the size of the TiO_2 and Y_2O_3 primary particles that constitute the granules (see Table 1), as it was observed, for example, by Vicent *et al* [27]. Moreover, this pore size value is optimal for granules uniaxial pressing, giving the granules an optimal crushability upon pressing [32]. Besides, Fig. 11 also shows that the presence of binder in the granules reduces the fraction of large pores, probably by sticking the solid particles stronger and closer to each other. It was also observed that as the suspension solid loading increases, the granule internal porosity becomes more finely distributed, as shown on Fig. 10. The same reasons as above are invoked to explain this phenomenon.

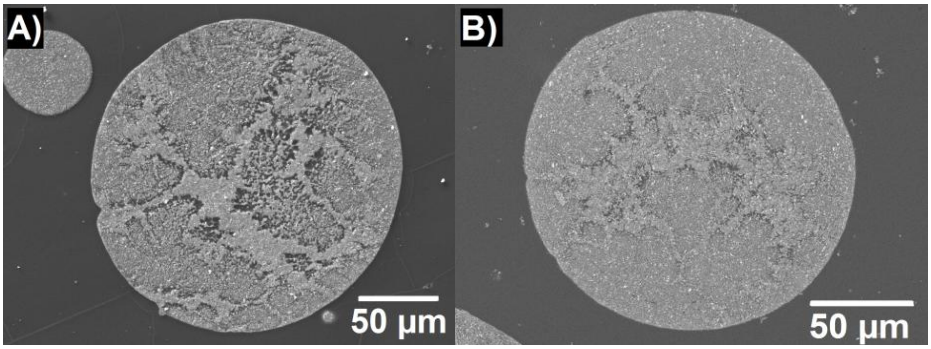

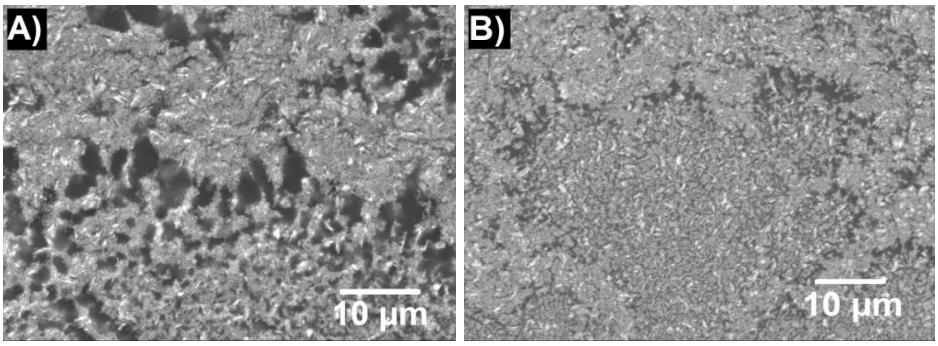

Fig. 10: Polished cross-sectional SEM views (2 magnifications each) of TiO_2-Y_2O_3 granules made by freeze granulation of suspensions containing A: 30 %v and B: 35 %v solid loading. Both suspensions also contain 0.75 wt% Darvan CN and 1 wt% PVA 22M.

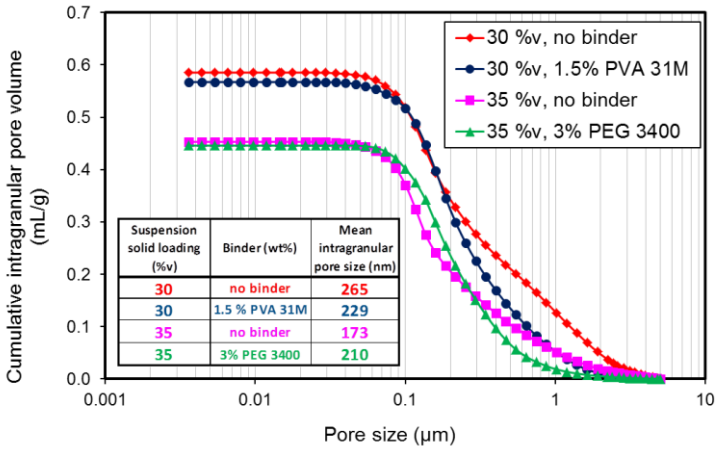

Fig. 11: Intragranular pore size distributions (mercury intrusion porosimetry) of TiO_2-Y_2O_3 granules obtained by freeze granulation of suspensions with various solid loadings and binder contents.

Chemical homogeneity of the granules was assessed by SEM-EDS cartography of granule polished cross section on Fig. 12. It appears that the yttrium and titanium elements are homogenously spread across all the volume of the granules obtained by freeze granulation. These granules do not exhibit segregation areas, indeed titanium and yttrium are both evenly distributed inside the granules. Higher magnification on the yttrium "spots" shown in the yttrium cartography of Fig. 12 indicated they are the size of the elementary particles present in the starting Y_2O_3 powder (about 1 to 2 µm). These results prove that:

- the two powders TiO_2 and Y_2O_3 are mixed in a very uniform and intimate way during the preparation of suspensions intended for freeze granulation,
- the uniform distribution between TiO_2 and Y_2O_3 is maintained during the freeze granulation,
- no particle migration happens during the freeze granulation process. Several authors made similar observations during studies on powder granulation using the freeze granulation process [3,4,6]. Causes of that phenomenon are explained above in the introduction part.

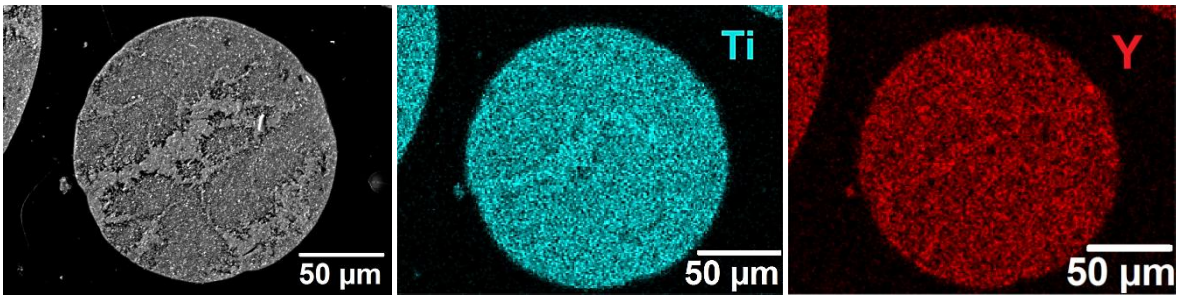

Fig. 12: SEM-EDS micrograph cross sectional view of a TiO_2-Y_2O_3 granule made from freeze granulation of suspension containing 35 %v solid, 0,75 wt% Darvan CN and 0.5 wt% PVA 22M. Titanium and yttrium EDS cartographies are depicted in blue and red, respectively.

Finally, granules flowability was evaluated in terms of Hausner ratio, which is determined by directly dividing the powder tapped density and the apparent density of the loosely packed powder bed. This method was chosen because it is quite simple and leads to reliable and reproducible findings as previously reported [33,34]. All the formulations tested yielded granules with Hausner ratios comprised between 1.02 and 1.12. Comparatively, in the literature, the flowability of powders intended for uniaxial pressing is considered good for Hausner ratios below 1.25 [18].

3.4 Granules pressing and sintering: pellet microstructure characterization

The TiO_2-Y_2O_3 freeze granulated powders previously prepared were uniaxially pressed to form pellets of about one centimeter both in diameter and height. Fig. 13 illustrates the compaction behavior of granules made from suspensions of different solid loadings. Granules from suspensions with the lowest solid loadings (25 and 30 %v solid) achieved maximal compaction at lower pressure (120-130 MPa) than granules made from suspensions with higher solid loadings (35 and 40 %v solid), that compact at higher pressure (190 MPa). This tendency can be linked to the granules mechanical strength, which is bound to the suspension solid loading, as previously highlighted by several authors [17,24,29]. Pressing pressures that were required were relatively low compared to those usually applied for uniaxial pressing, thanks to the good deformability and crushability of the granules formed by freeze granulation, as it has often been mentioned in the literature [2,18,29]. Finally, Fig. 13 also shows that the pellet green density is around 55% of the material theoretical density (confirmed by pellet dimension measurements by profilometer). This value is usual for green ceramics.

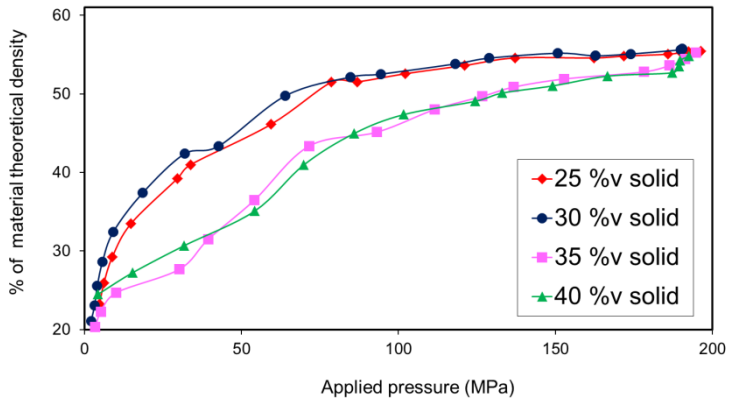

Fig. 13: Compaction during uniaxial pressing of TiO_2-Y_2O_3 granules (0.5 wt% Darvan CN, 1 wt% PEG 300) made from freeze granulation of suspensions with different solid loadings.

The green pellets that did not show any macroscopic external defects (see Fig. 14) were those made from formulations containing either:

- PVA (both 22M or 31M) in small amount (0.5 and 1 wt%),
- PEG of sufficient molecular weights (3400 and 6000 g/mol), used in larger amount (3 wt%),
- a mix of PVA (22M or 31M) and PEG (3400 or 6000) in equal proportions (50:50 PVA-to-PEG wt. ratio), at total amount of 1 wt%.

Moreover, green pellet fracture surface and polished cross section presented on Fig. 14 reveals that pellet internal structure is homogenous, dense and does not include flaws like large voids or cracks.

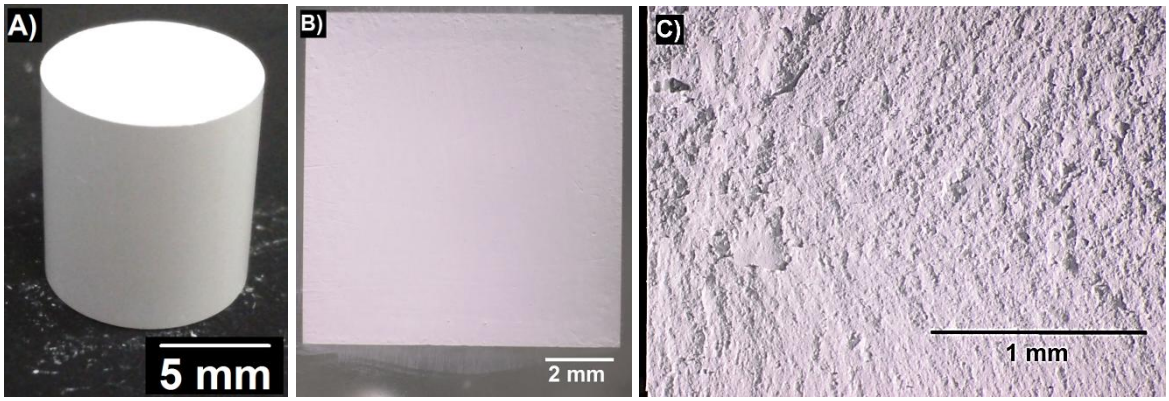

Fig. 14: Green TiO_2-Y_2O_3 pellet. A: overall view, B: polished cross section, C: fracture surface.

Subsequently, pellets were sintered in air at 1500°C for 1.5 hrs (heating rate 30°C/min) without debinding step. During sintering, solid-state reaction occurs between TiO_2 and Y_2O_3 to yield pyrochlore $Y_2Ti_2O_7$ [35]. The formation of this compound by total reaction was verified by XRD analysis on sintered pellet. The sintered density achieved is 94% of the theoretical density of the material. Polished cross sections of sintered pellet presented in Fig. 15 show that pellet microstructure displays homogenous repartition of yttrium and titanium elements, scattered across the pellet in micron-sized spots. A measurement of residual carbon concentration (LECO CS230 carbon analyzer) in the sintered pellets revealed that organic additives burnout was complete (carbon concentration below 25 ppm) despite the relatively fast sintering cycle and absence of debinding step.

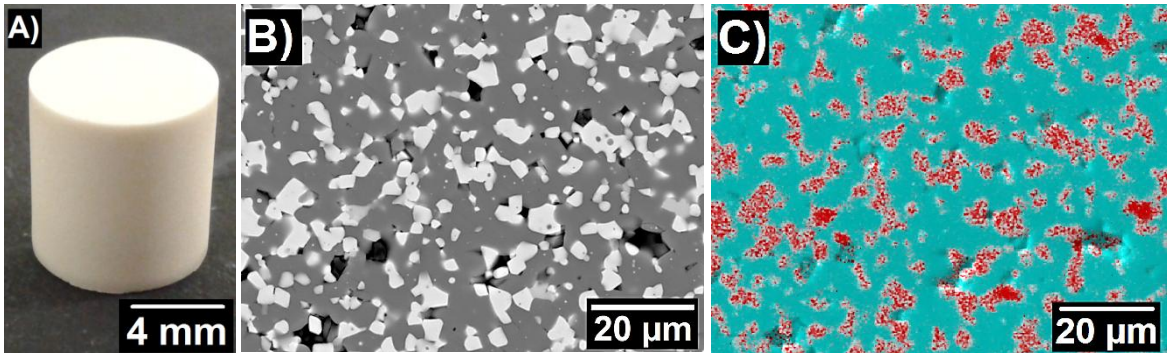

Fig. 15: Sintered TiO_2-Y_2O_3 pellet. A: overall view, B: polished cross section (SEM), C: polished cross section SEM-EDS cartography (yttrium depicted in red, titanium in blue).

4. Conclusion and perspectives

In this paper, TiO_2-Y_2O_3 granules were made from micron-sized TiO_2 and Y_2O_3 commercial powders. Granulation of these mixed powders was performed with the freeze granulation process of water-based powder suspensions. This granulation process was studied and optimized to ensure the production of TiO_2-Y_2O_3 granules that are physically and chemically homogenous, highly flowable (through the control of the granule morphology/sphericity and surface aspect) and monomodaly sized (200-300 µm) without fines. To that end, atomization conditions during freeze granulation (gas and suspension flow rates) and suspension formulation (solid loading, viscosity and presence of binders) were studied. It was proven that atomization conditions mostly influence granule size distribution and morphology. Moreover, suspension solid loading influences granules size, surface aspect and porosity. Finally, binder nature and concentration influences granule surface aspect and size distribution.
From these granules, pellets were formed by uniaxial pressing. The above-mentioned optimal characteristics of the granules allowed the formation of flaw-free, resistant and homogenous TiO_2-Y_2O_3 pellets. In particular, granules high flowability and crushability allowed the pressing of homogeneous green pellets at low pressures. Moreover, this study has also spotlighted the role and effects of several binders (nature and concentration used) on green pellets surface aspect and resistance against chipping/cracking.
These pellets presented a satisfying sinterability, despite the presence of the organic additives used for the granulation and shaping process. However, their sinterability could probably be improved by optimizing the sintering cycle (heating rate and debinding step). The good yttrium-titanium homogeneity of the sintered pellets testifies of the good suspension dispersion.
The next step will consist in replacing the TiO_2 and Y_2O_3 surrogate powders by the corresponding radioactive powders (respectively UO_2 and PuO_2). The feedback and knowledge acquired with the investigations on surrogate powders will benefit to the transposition of the freeze granulation process to the production of MOX pellets.

Acknowledgements

This study is supported by the *Commissariat à l'Energie Atomique* (CEA) in partnership with the Institute of Research for Ceramics (IRCER). The authors are thankful to P. Duport and S. Blanchet from the IRCER Limoges and J-P. Bayle from the CEA Marcoule for the technical help and advice provided during experiments.

References

[1] D. Haas, A. Vandergheynst, J. van Vliet, R. Lorenzelli, JL. Nigon. Mixed-oxide fuel fabrication technology and experience at the Belgonucléaire and CFCa plants and further developments for the MELOX plant. *Nucl. Technol.* 106 (1994) 60-82.

[2] V. Tsakaloudi, G. Kogias, V. Zaspalis. Freeze granulation: a novel technique for low-loss Mn-Zn ferrites. International Magnetics Conference 2008 (INTERMAG 2008), Madrid, Spain, 2008.

[3] J. Orlenius, O. Lyckfeldt, KA. Kasvayee, P. Johander. Water based processing of $LiFePO_4$/C cathode material for Li-ion batteries utilizing freeze granulation. *J. Power Sources* 213 (2012) 119-127.

[4] K. Rundgren, O. Lyckfeldt, M.Sjöstedt. Improving powders with freeze granulation. Ceramic Industry (2003) 40-44.

[5] W.J. Walker Jr, J.S. Reed. Influence of slurry parameters on the characteristics of spray-dried granules. *J. Am. Ceram. Soc.* 82 (1999) 1711–19.

[6] B. Nyberg, E. Carlström, R. Carlsson. Granulation of ceramic powders for pressing by spray-freezing and freeze-drying. EuroCeramics II, vol. 1, Deutsche Keramische Gesellschaft, pp. 447- 451, 1993.

[7] K. Rundgren, O. Lyckfeldt, M. Sjöstedt. Freeze granulation for the processing of silicon nitride ceramics. *Key Eng. Mater.* 264-268 issue I (2004), issue I, 281-284.

[8] SM. Olhero, JMF. Ferreira. Influence of particle size distribution on rheology and particle packing of silica-based suspensions. *Powder Technol.* 139 (2004) 69–75.

[9] R. Greenwood, PF. Luckham, T. Gregory. The effect of diameter ratio and volume ratio on the viscosity of bimodal suspensions of polymer lattices. *J. Colloid Interface Sci.* 191 (1997) 11 –21.

[10] A.U. Khan, B.J. Briscoe, P.F. Luckham. Interaction of binders with dispersant stabilised alumina suspensions. *Colloids Surf., A* 161 (2000) 243–257.

[11] B.J. Briscoe, A.U. Khan, P.F. Luckham. Optimising the dispersion on an alumina suspension using commercial polyvalent electrolyte dispersants. *J. Eur. Ceram. Soc.* 14 (1998) 2141-2147.

[12] M. Olsson, A.M. Jakobsson, Y. Albinsson. Surface charge densities of two actinide (IV) oxides: UO_2 and ThO_2. *J. Colloid Interface Sci.* 256 (2002) 256–261.

[13] M. Kosmulski. Compilation of PZC and IEP of sparingly soluble metal oxides and hydroxides from literature. *Adv. Colloid Interface Sci.* 152 (2009) 14-25.

[14] IS. Bouhaik, P. Leroy, P. Ollivier, M. Azaroual, L. Mercury. Influence of surface conductivity on the apparent zeta potential of TiO_2 nanoparticles: application to the modeling of their aggregation kinetics. *J. Colloid Interface Sci.* 406 (2013) 75–85.

[15] R. Sprycha, J. Jablonski, E. Matijevic. Zeta potential and surface charge of monodispersed colloidal yttrium(III) oxide and basic carbonate. *J. Colloid Interface Sci.* 149 (1992) 561-568.

[16] F. La Lumia, L. Ramond, C. Pagnoux, G. Bernard-Granger. Preparation and co-dispersion of TiO_2-Y_2O_3 suspensions through the study of their rheological and electrokinetic properties. *Ceram. Int*. 2018

[17] B.P.C. Raghupathy, J.G.P. Binner. Spray freeze drying of YSZ nanopowder. *J. Nanopart. Res.* 14 (2012) 921-936.

[18] M. Stuer, Z. Zhao, P. Bowen. Freeze granulation: Powder processing for transparent alumina applications. *J. Eur. Ceram. Soc.* 32 (2012) 2899–2908.

[19] S. Liufu, H. Xiao, Y. Li Investigation of PEG adsorption on the surface of zinc oxide nanoparticles. *Powder Technol.* 145 (2004) 20– 24.

[20] U. Paik, V.A. Hackley, H-W. Lee. Dispersant–binder interactions in aqueous silicon nitride suspensions. *J. Am. Ceram. Soc.* 82 (1999) 833–40.

[21] P.C. Hidber, T.J. Graule, L.J. Gauckler. Competitive adsorption of citric acid and poly(viny1 alcohol) onto alumina and its influence on the binder migration during drying. *J. Am. Ceram. Soc.* 78 (1995) 1775-80.

[22] P. Jenkins, M. Snowden. Depletion flocculation in colloidal dispersions. *Adv. Colloid Interface Sci*. 68 (1996) 57-96.

[23] Y. Zhang, J. Binner, C. Rielly, B. Vaidhyanathan. Comparison of spray freeze dried nanozirconia granules using ultrasonication and twin-fluid atomization. *J. Eur. Ceram. Soc.* 34 (2014) 1001–1008.

[24] P. Barick, B.P. Saha, S.V. Joshi, R. Mitra. Spray-freeze-dried nanosized silicon carbide containing granules: Properties, compaction behaviour and sintering. *J. Eur. Ceram. Soc.* 36 (2016) 3863–3877.

[25] I.C. Kemp, R. Wadley, T. Hartwig, U. Cocchini, Y.S. Toh, L. Gorringe *et al*. Experimental study of spray drying and atomization with a two-fluid nozzle to produce inhalable particles. *Drying Technol*. 8 (2013) 930–941.

[26] K. Yan, Z. Ning, M. Lü, C. Sun. Study on droplet size and velocity distributions of a pressure swirl atomizer based on the maximum entropy formalism. *Entropy* 17 (2015) 580-593.

[27] M. Vicent, E. Sánchez, T. Molina, M.I. Nieto, R. Moreno. Comparison of freeze drying and spray drying to obtain porous nanostructured granules from nanosized suspensions. *J. Eur. Ceram. Soc.* 32 (2012) 1019–1028.

[28] W. Liu, Z. Xie. Spray Freeze Granulation of submicron alumina and its sintering behavior via spark plasma sintering. *Sci. Sintering* 47 (2015) 279-288.

[29] T. Moritz, A. Nagy. Preparation of super soft granules from nanosized ceramic powders by spray freezing. *J. Nanopart. Res.* 4 (2002) 439–448.

[30] A. Wajler, H. Weglarz, A. Sidorowicz, L. Zych, M. Nakielska, K. Jach *et al*. Preparation of transparent neodymium-doped yttrium aluminate garnet (Nd:YAG) ceramics with the use of freeze granulation. Opt. Mater. 50 (2015) 40–46.

[31] E. Adolfsson, Z. Shen. Effects of granule density on strength and granule related defects in zirconia. *J. Eur. Ceram. Soc.* 32 (2012) 2653–2659.

[32] H. Kamiya., K. Isomura, G. Jimbo, T. Jun-ichiro. Powder processing for the fabrication of Si_3N_4 ceramics: I, Influence of spray-dried granule strength on pore size distribution in green compacts. *J. Am. Ceram. Soc.* 78 (1995) 49-57.

[33] M. Vicent, E. Sánchez, I. Santacruz, R. Moreno. Dispersion of TiO_2 nanopowders to obtain homogeneous nanostructured granules by spray-drying. *J. Eur. Ceram. Soc.* 31 (2011) 1413–19.

[34] E. Sánchez, M. Vicent, A. Moreno, M.D. Salvador, E. Klyastina, V. Bonache *et al*. Preparation and spray-drying of nanoparticle Al_2O_3-TiO_2 suspensions to obtain nanostructures coatings by APS. *Surf. Coat. Technol.* 205 (2010) 987–92.

[35] W. Gong, D. Li, Z. Chen, F. Zheng, Y. Liu, Y. Du *et al*. Phase equilibria of the TiO_2-Y_2O_3 system. *CALPHAD* 33 (2009) 624-27.